

Research Paper

# Bivalent inhibition of human $\beta$ -tryptase

Norbert Schaschke <sup>a</sup>, Gabriele Matschiner <sup>b</sup>, Frank Zettl <sup>b</sup>, Ulf Marquardt <sup>a</sup>,  
Andreas Bergner <sup>a,1</sup>, Wolfram Bode <sup>a</sup>, Christian P. Sommerhoff <sup>b</sup>, Luis Moroder <sup>a,\*</sup>

<sup>a</sup>Max-Planck-Institut für Biochemie, Am Klopferspitz 18a, D-82152 Martinsried, Germany

<sup>b</sup>Abteilung für Klinische Chemie und Klinische Biochemie, Chirurgische Klinik und Poliklinik Innenstadt der LMU München, D-80336 Munich, Germany

Received 24 November 2000; revisions requested 19 January 2001; revisions received 8 February 2001; accepted 9 February 2001

First published online 22 February 2001

## Abstract

**Background:** Human  $\beta$ -tryptase is a mast cell specific trypsin-like serine protease that is thought to play a key role in the pathogenesis of diverse allergic and inflammatory disorders like asthma and psoriasis. The recently resolved crystal structure revealed that the enzymatically active tetramer consists of four quasi-identical monomers. The spatial display of the four identical active sites represents an ideal basis for the rational design of bivalent inhibitors.

**Results:** Based on modeling experiments homobivalent inhibitors were constructed using (i) 6A,6D-dideoxy-6A,6D-diamino- $\beta$ -cyclodextrin as a rigid template to bridge the space between the two pairs of identical active sites and (ii) 3-(aminomethyl)benzene as a headgroup to occupy the arginine/lysine specific S1 subsites. A comparative analysis of the inhibitory potencies of synthetic constructs that differ in size and type of the spacer between headgroup and template revealed that the construct contained two 3-(aminomethyl)benzenesulfonyl-glycine groups linked to the

6A,6D-diamino groups of  $\beta$ -cyclodextrin as an almost ideal bivalent inhibitor with a cooperativity factor of 1.9 vs. the ideal value of 2. The bivalent binding mode is supported by the inhibitor/tetramer ratio of 2:1 required for inactivation of tryptase and by X-ray analysis of the inhibitor/tryptase complex.

**Conclusion:** The results obtained with the rigid cyclodextrin template underlined the importance of a minimal loss of conformational entropy in bivalent binding, but also showed the limitations imposed by such rigid core molecules in terms of optimal occupancy of binding sites and thus of enthalpic strains in bidentate binding modes. The main advantage of bivalent inhibitors is their high selectivity for the target enzyme that can be achieved utilizing the principle of multivalency. © 2001 Elsevier Science Ltd. All rights reserved.

**Keywords:**  $\beta$ -Tryptase; Bivalent inhibitor;  $\beta$ -Cyclodextrin; Circular dichroism; X-ray analysis

## 1. Introduction

Cooperativity plays a central role in folding pathways of biomolecules into higher order structures as well as in

molecular recognition that leads to biological functions. It is typically employed when numerous weak interactions operate simultaneously leading to polyvalent intermolecular interactions, which are responsible for the selectivity and avidity of protein/protein or protein/carbohydrate recognition and thus drive the unidirectional reactions in biochemical cascades [1]. By mimicking nature, this principle of polyvalency has been largely exploited to modulate carbohydrate/protein interactions [2,3] and particularly in the design of inhibitors of adhesion processes, e.g. of pathogens to cell membranes [4–7]. It has also been applied in the control of cellular signal transduction [8–10] and in the development of enzyme inhibitors [11–15].

The physical laws that govern such polyvalent binding of biomolecules have been the object of extensive studies [1,16–18]. Usually, the contributions of the single binding subsites to the overall free energy of binding are rationalized in terms of their intrinsic binding energies and of a

*Abbreviations:* DMF, *N,N*-dimethylformamide; THF, tetrahydrofuran; DIEA, *N,N*-diisopropylethylamine; TFA, trifluoroacetic acid; PyBOP, benzotriazol-1-yloxy-tris(pyrrolidino)-phosphonium hexafluorophosphate; Boc, *tert*-butoxycarbonyl; (Boc)<sub>2</sub>O, di-*tert*-butyl dicarbonate; PPh<sub>3</sub>, triphenylphosphine; HOBt, 1-hydroxybenzotriazole; EDC, *N*-ethyl-*N'*-(3-dimethylaminopropyl)-carbodiimide hydrochloride; CD, circular dichroism; TLC, thin layer chromatography; HPLC, high performance liquid chromatography; ESI-MS, electrospray ionization mass spectrometry

<sup>1</sup> Present address: CCDC, 12 Union Road, Cambridge CB2 1EZ, UK.

\* Correspondence: Luis Moroder;  
E-mail: moroder@biochem.mpg.de

connection Gibbs energy that represents the change in the probability of binding that results from the assembly of the binding subsites into one molecule [18]. Quantification of these contributions is particularly difficult in heteropolyvalency. Therefore, homo-polyvalent ligands interacting with identical binding subsites of the receptor molecule in well defined systems are required to gain a better insight into the thermodynamics of such molecular recognition processes. Recently, a well defined system consisting of a homotrimeric vancomycin construct that binds to a homotrimeric ligand was utilized to confirm the approximate additivity of the free binding energies [19,20].

In terms of multivalent enzyme inhibition, until recently only the thrombin/hirudin complex was known whose X-ray structure clearly revealed two distinct domain interactions at the active site and the fibrinogen binding site, respectively [21]. By exploiting this information, highly potent hirudin mimetics, e.g. the hirulogs [13], were developed. These hetero-bivalent inhibitors bind to the two different subsites simultaneously, thus leading to a strong potentiation of affinity and selectivity. With the discovery of multicatalytic protease complexes and particularly with the X-ray structure analyses of the eukaryotic proteasome and human  $\beta$ -tryptase [22–24], two interesting new target molecules have become available with (pairwise) identical multiple active sites displayed spatially in a defined geometrical order. This type of architecture of the receptor molecule is ideally suited for the design of synthetic inhibitors based on the principle of oligovalency and for investigating potential limitations for the additivity of the free binding energies caused by the chemical structure of the bivalent ligands.

The 20S proteasome from *Saccharomyces cerevisiae* exhibits a cylindrical architecture in which the 28 subunits are assembled as an  $(\alpha 1\text{--}\alpha 7, \beta 1\text{--}\beta 7)_2$  complex consisting of four stacked heptameric rings with a spatial arrangement of two sets of three different active sites in a geometrical array [22]. Due to the bottleneck of the proteasome entrance that recruits from outside only fully unfolded linear proteins for digestion and thus significantly restricts the choice of spacers, in a previous study we used polyoxyethylene (PEG) of appropriate size to crosslink pairwise the tripeptide aldehydes H-Leu-Leu-Nle-H and H-Arg-Val-Arg-H as headgroups for the chymotryptic  $\beta 5/\beta 5'$  and tryptic  $\beta 2/\beta 2'$  active site pairs, respectively [25,26]. Although highly selective inhibition of the chymotrypsin- and trypsin-like activities of the proteasome was achieved with such constructs, the potency was increased by only two orders of magnitude compared to the monovalent inhibitors. This relatively small gain in free binding energy by the bivalent inhibitors has to be attributed to the high degree of flexibility of the spacer and thus to the loss of conformational entropy associated with the bidentate interaction that makes binding at the second site energetically less favored.

Differently from the proteasome, the human  $\beta$ -tryptase

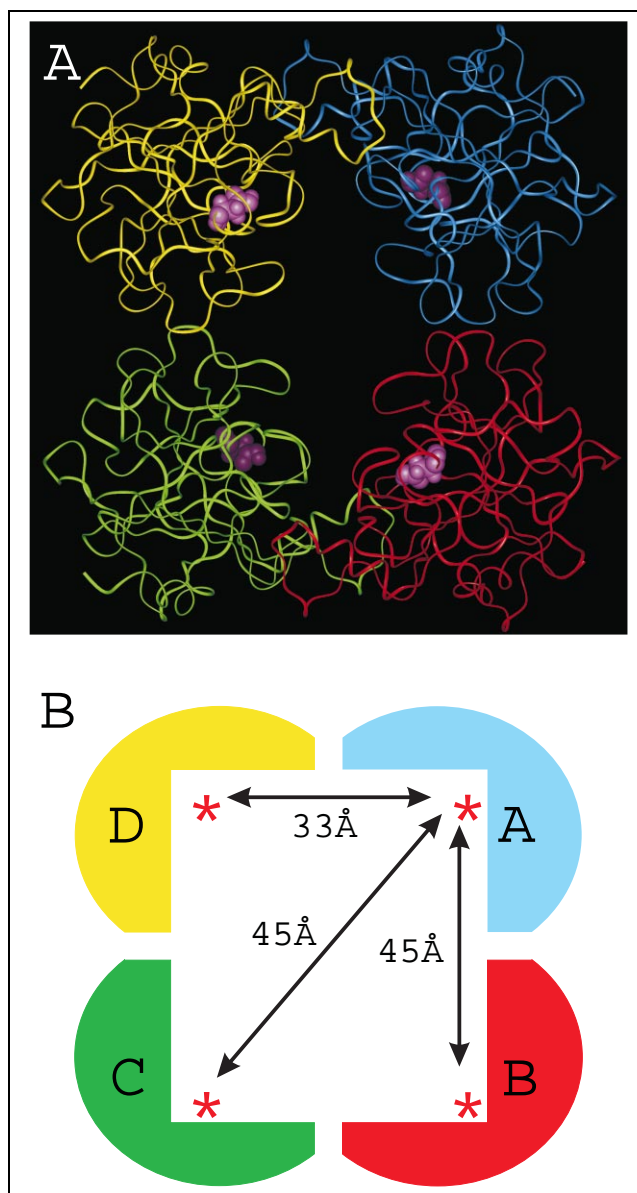


Fig. 1. (A) Ribbon representation of the  $\beta$ -tryptase tetramer. The subunits A, B, C, and D are colored blue, red, green, and yellow, respectively; Asp-189 at the bottom of each S1 pocket is shown as magenta CPK representation. (B) Schematic representation of the tryptase tetramer with inter-S1 subsite distances. Asp-189 at the bottom of each S1 pocket is shown as a red asterisk.

tetramer consists of four identical subunits which according to X-ray analysis are assembled in a structurally quasi-equivalent form into a flat ring, with the four active sites pointing towards an oval central pore [23,24]. This array of active sites, schematically outlined in Fig. 1, restricts the access of macromolecular substrates to the digestion chamber and prevents inhibition of the enzyme by all known endogenous proteinase inhibitors [27]. However, the relatively large size of the open central pore should allow free access of even complex synthetic constructs to the active sites and thus the use of both flexible and rigid

spacers for the rational design of homobivalent and ultimately even of homotetravalent inhibitors.

In view of this unique tetrameric architecture of the tryptase, in the present study we have investigated the effects of flexible and rigid templates on the affinity of bivalent inhibitors. As expected, rigid spacers proved to be highly superior to flexible ones, but the study also confirmed that optimal fitting of the binding headgroups is required when utilizing such templates in order to avoid enthalpic binding strain which can offset the gain in entropy, and thus energetically disfavor bivalent binding.

## 2. Results

### 2.1. Design of bivalent $\beta$ -tryptase inhibitors

The trypsin-like specificity of  $\beta$ -tryptase is due to the Asp-189 residue positioned at the bottom of the S1 subsite which accommodates and binds preferentially arginine/lysine residues or related mimetics as confirmed by the X-ray structure of the  $\beta$ -tryptase/4-amidinophenyl pyruvate complex [23,24]. The spatial arrangement of the four S1 subsites is shown in Fig. 1. The shortest distance between the side chain carboxylates of the Asp-189 residues of two neighboring S1 subsites is that between the subunits A/D and B/C and corresponds to approximately 33 Å, whereas the distance between the S1 subsites of the subunits A/C and B/D as well as of A/B and D/C is approximately 45 Å. To avoid hydrophobic collapses of the spacer/template on the protein surface of the inner cavity and taking into account the bulk water that occupies the central pore of the tryptase tetramer, hydrophilic spacers of due size appeared to be the most suitable candidates for the design of bivalent ligands. Correspondingly, in the present study PEG and carbohydrate molecules were used to construct double-headed inhibitors capable of spanning the distance between two of the four active sites of the tetramer.

### 2.2. Homobivalent inhibitors with PEG as spacer

The trypsin-like active sites of the  $\beta$ -tryptase tetramer are efficiently inhibited by peptidyl arginals as confirmed by the  $K_i$  value of the tripeptide aldehyde Ac-Arg-Val-Arg-H (**1**) (Table 1) previously synthesized as a monovalent inhibitor of the trypsin-like active sites of the proteasome [25,26]. For a bivalent inhibition of the proteasome, the amino-free compound **1** was crosslinked with a

Table 1  
Inhibition of the  $\beta$ -tryptase tetramer by PEG-linked mono- and bivalent inhibitors

Compound	Structure	$K_i$ (nM)
<b>1</b>	Ac-Arg-Val-Arg-H	15
<b>2</b>	HOOC-PEG-CO-Arg-Val-Arg-H	36
<b>3</b>	H-Arg-Val-Arg-OC-PEG-CO-Arg-Val-Arg-H	1.6

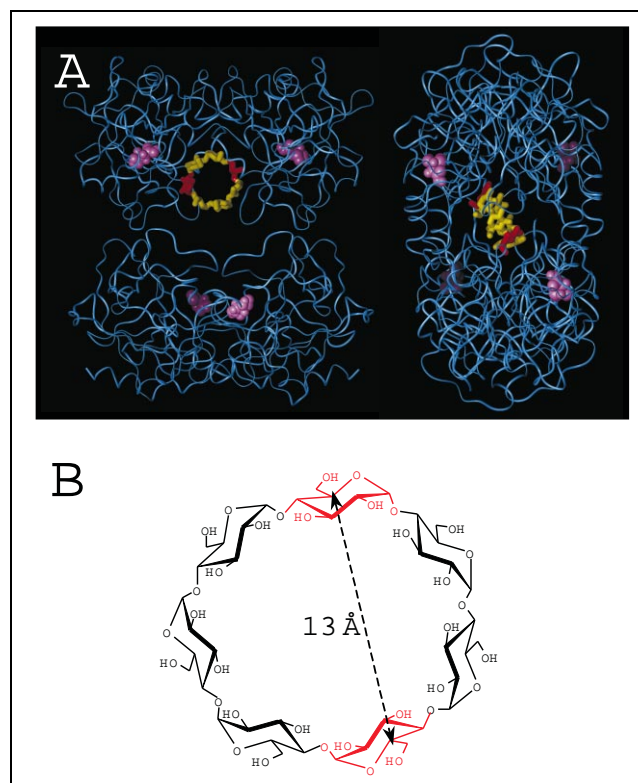
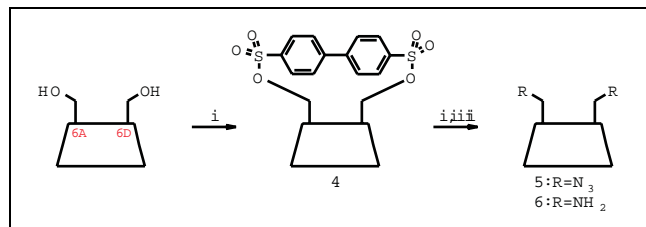


Fig. 2. (A) Ribbon representation of the  $\beta$ -tryptase tetramer with  $\beta$ -cyclodextrin positioned in the central pore between the tryptase subunits A and D. Asp-189 at the bottom of each S1 pocket is shown as magenta CPK representation,  $\beta$ -cyclodextrin in stick representation, and the sugar units A and D are colored red. (B) Structure of  $\beta$ -cyclodextrin; the sugar units A and D are colored red.

(PEG)<sub>19–25</sub> polymer to span a distance of 50 Å and more. Although largely oversized for the shorter inter-S1 subsite distance of 33 Å and to a lesser extent for the larger inter-S1 subsite distance of 45 Å of the tetramer, the flexible and highly hydrated bivalent construct **3** was analyzed for its inhibitory potency. A relatively low increase in potency by only a factor of approximately 10 was obtained with compound **3** as compared to the monovalent inhibitor **1**. A potential interference by the large PEG chain can be excluded, as the inhibitory activity of the pegylated peptide aldehyde **2** is reduced only by a factor of 2.

### 2.3. Homobivalent inhibitors with $\beta$ -cyclodextrin as spacer

As an alternative to the PEG spacer, carbohydrate-based core structures were analyzed in modeling experiments as appropriate water-solvated templates. The latter property was expected to reduce the solvation effect on the binding energies at least concerning the linker moiety to a minimum. Among the various carbohydrates inspected,  $\beta$ -cyclodextrin emerged as an ideally sized spacer (Fig. 2).  $\beta$ -Cyclodextrin consists of seven  $\alpha$ -D-glucose units (A–G) which are linked in an  $\alpha$ -glycosidic (1  $\rightarrow$  4) manner. The primary hydroxy groups of the sugar units A and D



Scheme 1. Synthesis of 6A,6D-diamino-6A,6D-dideoxy-β-cyclodextrin (**6**). Reaction conditions: (i) biphenyl-4,4'-disulfonyl chloride, pyridine; (ii)  $\text{NaN}_3$ , *N,N*-dimethylformamide (DMF); (iii) triphenylphosphine ( $\text{PPh}_3$ ), then 25% aqueous ammonia, DMF.

are pointing towards the S1 subsites of the adjacent A/D and B/C subunits in a manner particularly suitable for a bivalent presentation of binding headgroups. As the space bridged by the β-cyclodextrin is 13 Å, this rigid core molecule was expected to greatly reduce the loss of conformational entropy of a bivalent ligand upon binding of the headgroups. Moreover, based on modeling experiments an easy access of this cyclic carbohydrate into the central cavity of the tetrameric protease complex was expected. From a previous use of β-cyclodextrin as carrier of peptide hormones and inhibitors we also knew that, if sufficiently spaced from the ligand, the cyclic heptaamylose does not interfere with their recognition and binding to receptor molecules [28–30].

Docking experiments of various arginine mimetics to the S1 subsites of β-tryptase as well as our own experi-

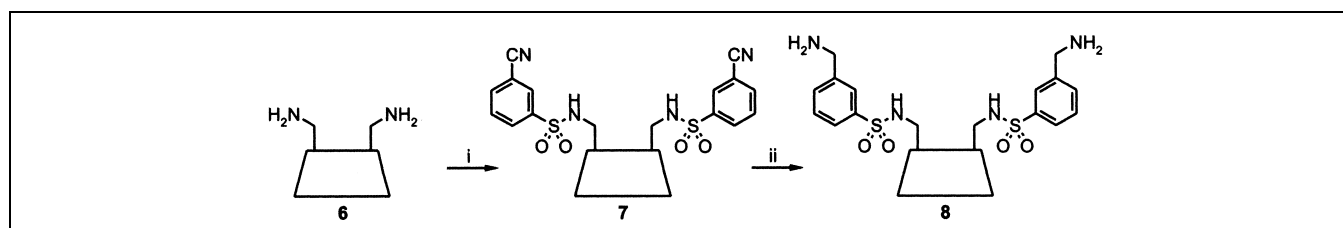
mental results with synthetic inhibitors (unpublished results) indicated a preferred binding of *m*- over *p*-substituted benzenesulfonyl derivatives and an optimal fit of headgroups of the type 3-(aminomethyl)benzenesulfonyl when grafted onto the two distal positions A and D of β-cyclodextrin via relatively short spacers.

#### 2.4. Synthesis of β-cyclodextrin-based inhibitors

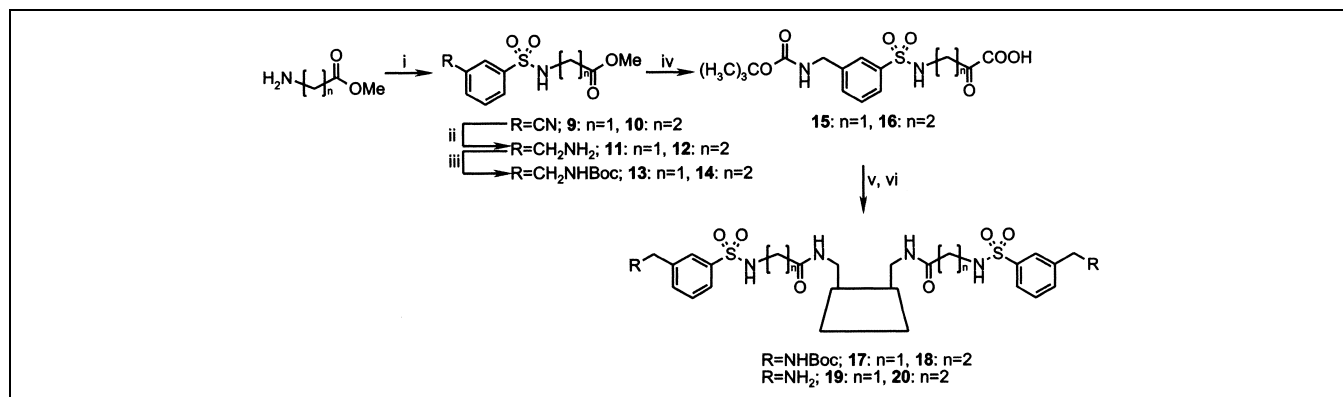
To functionalize appropriately β-cyclodextrin at the primary hydroxy functions within units A and D, this cyclic carbohydrate molecule was converted to 6A,6D-diamino-6A,6D-dideoxy-β-cyclodextrin (**6**) adopting the procedure of Tabushi et al. [31] (Scheme 1). The diamine **6** then served for the production of various bivalent compounds containing two 3-(aminomethyl)benzenesulfonyl moieties grafted onto the template with or without spacers (Schemes 2 and 3).

To analyze the potential effects of the template on the binding of headgroups to the S1 pocket of β-tryptase, β-cyclodextrin was monofunctionalized as the *per*-acetyl-6-amino-6-deoxy-β-cyclodextrin derivative **21** essentially as described previously [28], and was then used for the synthesis of the monovalent inhibitor **24** as shown in Scheme 4.

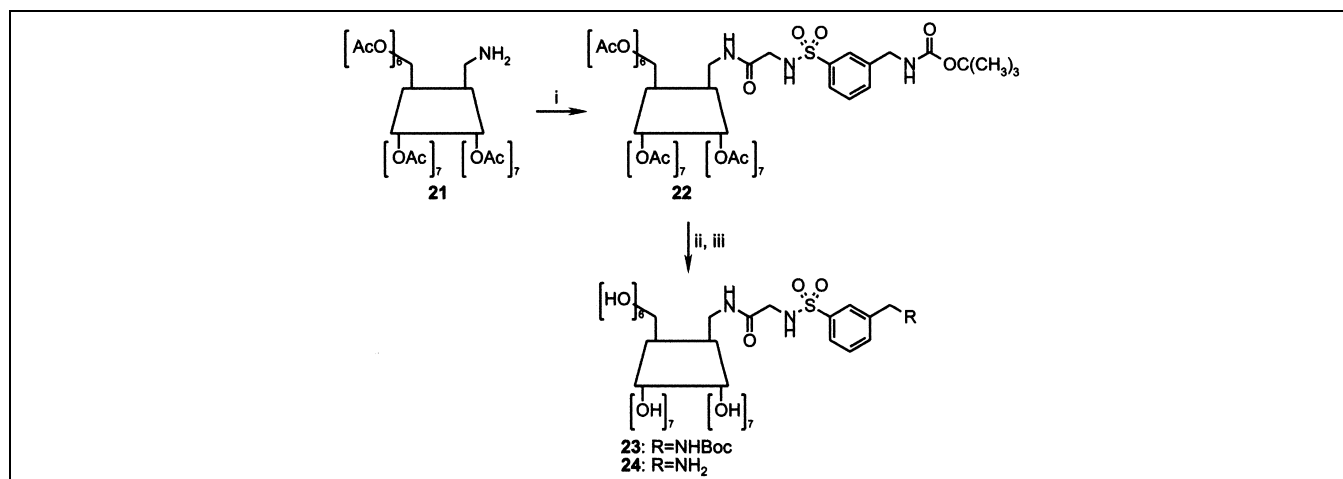
Finally, to assess the effect of the pyramidal sulfonamide group on the inhibitory potency of the bivalent constructs, it was replaced by the planar carboxamide group



Scheme 2. Synthesis of 6A,6D-bis[3-(aminomethyl)benzenesulfonylamino]-6A,6D-dideoxy-β-cyclodextrin (**8**). Reaction conditions: (i) 3-cyanobenzenesulfonyl chloride/ $\text{NaOH}$ ,  $\text{H}_2\text{O}$ /acetonitrile; (ii)  $\text{H}_2$ /10% Pd-C, 90% aqueous AcOH.



Scheme 3. Synthesis of 6A,6D-bis[3-(aminomethyl)benzenesulfonyl-glycyl-amino]-6A,6D-dideoxy-β-cyclodextrin (**19**) and 6A,6D-bis[3-(aminomethyl)benzenesulfonyl-β-alanyl-amino]-6A,6D-dideoxy-β-cyclodextrin (**20**);  $n = 1$ : glycine;  $n = 2$ : β-alanine. Reaction conditions: (i) 3-cyanobenzenesulfonyl chloride/ $\text{NaHCO}_3$ ,  $\text{H}_2\text{O}/\text{CHCl}_3$ ; (ii)  $\text{H}_2$ /10% Pd-C, AcOH; (iii) di-*tert*-butyl dicarbonate ( $(\text{Boc})_2\text{O}$ )/ $\text{NaHCO}_3$ , dioxane/ $\text{H}_2\text{O}$  (1:1); (iv) 1 N NaOH, tetrahydrofuran (THF); (v) **6**/benzotriazol-1-yloxy-tris(pyrrolidino)-phosphonium hexafluorophosphate (PyBOP)/*N,N*-diisopropylethylamine (DIEA), DMF; (vi) 90% aqueous trifluoroacetic acid (TFA).



Scheme 4. Synthesis of 6-[3-(aminomethyl)benzenesulfonyl-glycylamino]-6-deoxy- $\beta$ -cyclodextrin (**24**). Reaction conditions: (i) 15/*N*-ethyl-*N'*-(3-dimethylaminopropyl)-carbodiimide hydrochloride (EDC)/1-hydroxybenzotriazole (HOBt),  $\text{CHCl}_3$ ; (ii) 1 N NaOH, MeOH/ $\text{H}_2\text{O}$ ; (iii) 90% aqueous TFA.

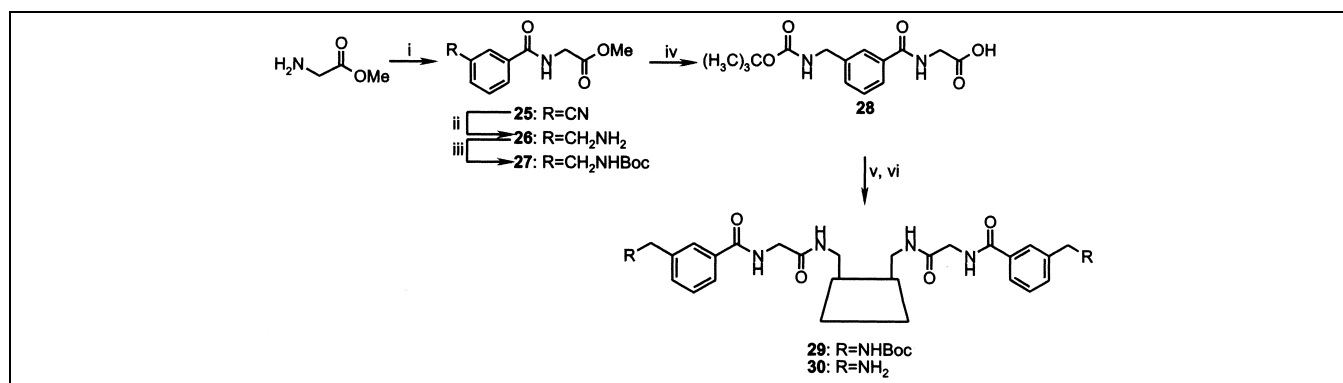
using 3-(*tert*-butoxycarbonylamino)benzoyl-glycine (**28**) to bis-acylate via the PyBOP procedure [32] 6*A*,6*D*-diamino-6*A*,6*D*-dideoxy- $\beta$ -cyclodextrin (**6**) and to produce upon acidolytic deprotection the bis-basic compound **30** (Scheme 5).

#### 2.5. Inhibition of $\beta$ -tryptase by $\beta$ -cyclodextrin-based inhibitors

The critical effect of the spacer between the headgroup 3-(aminomethyl)benzenesulfonyl and the  $\beta$ -cyclodextrin template is reflected in the inhibition constants of the various bivalent constructs listed in Table 2. Without spacer the  $K_i$  value of the bivalent inhibitor **8** was found to be almost identical to that of the headgroup 3-(aminomethyl)benzenesulfonyl-glycine methyl ester (**11**) ( $K_i$  30 and 17  $\mu\text{M}$ , respectively). This clearly shows that this inhibitor **8** is not able to interact with two neighboring S1 subsites

simultaneously and therefore behaves like a monovalent inhibitor. Conversely, with glycine as spacer, i.e. with compound **19**, a more than  $10^4$ -fold increase in inhibitory potency was obtained when compared to the headgroup **11**, thus strongly supporting a bidentate binding to the tetrameric protease. An increase of the spacer length by a methylene moiety in compound **20**, as produced by replacing the glycine with a  $\beta$ -alanine residue, is sufficient to reduce the inhibition potency to some extent. Thus, with glycine as spacer apparently the optimal spacer size was achieved, unless the additional rotor introduced with the methylene group leads to an entropic penalty in terms of loss of conformational entropy.

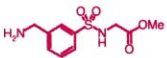
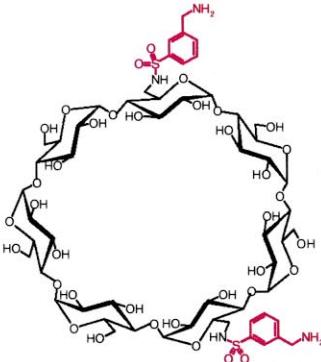
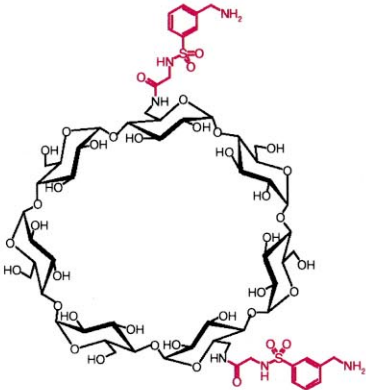
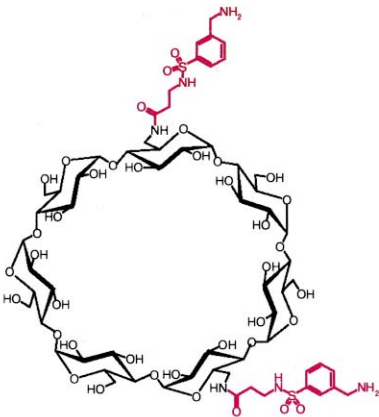
The high degree of selectivity of  $\beta$ -tryptase inhibition by the bivalent inhibitor **19** versus trypsin and thrombin is reflected by the  $K_i$  values reported in Table 3. As expected from a simple occupation of the S1 subsite, the headgroup **11** is a poor inhibitor of all three enzymes, and both its



Scheme 5. Synthesis of 6,6'-bis[3-(aminomethyl)benzoyl-glycyl-amino]-6,6'-dideoxy- $\beta$ -cyclodextrin (**30**). Reaction conditions: (i) 3-cyanobenzoyl chloride/ $\text{NaHCO}_3$ ,  $\text{H}_2\text{O}/\text{CHCl}_3$ ; (ii)  $\text{H}_2$ /10% Pd-C, AcOH; (iii)  $(\text{Boc})_2\text{O}/\text{NaHCO}_3$ , dioxane/ $\text{H}_2\text{O}$  (1:1); (iv) 1 N NaOH, THF; (v) **6**/PyBOP/DIEA, DMF; (vi) 90% aqueous TFA.

Table 2

Inhibition of the  $\beta$ -tryptase tetramer by  $\beta$ -cyclodextrin-based bivalent inhibitors: influence of the spacer length on the inhibitory potency

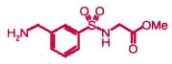
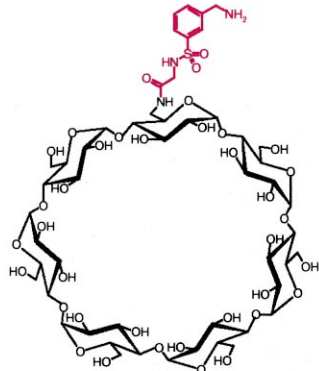
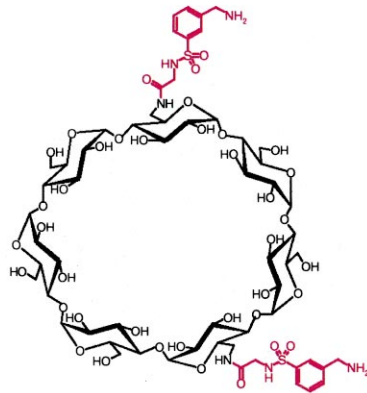
Compound	Structure	Spacer Length	$K_i$ [ $\mu$ M]
		[Number of Atoms]	
11		---	17
8		0	30
19		3	0.0006
20		4	0.0025

mono- and bis-presentation by the cyclodextrin template does not significantly alter the affinity for trypsin and thrombin. Thus exploiting the low affinity of the head-group for trypsin-like enzymes, with the bivalent inhibitor

**19** a more than  $10^4$ -fold selectivity for  $\beta$ -tryptase was achieved. As already expected from the inhibitory activity of construct **8**, the  $\beta$ -cyclodextrin moiety itself only slightly affects the affinity of the headgroup for tryptase as well as

Table 3

Inhibition of  $\beta$ -tryptase, trypsin, and thrombin by  $\beta$ -cyclodextrin-based mono- and bivalent inhibitors: influence of the cyclodextrin moiety on the inhibitory potency

Compound	Structure	Tryptase	Trypsin	Thrombin
$K_i$ [ $\mu$ M]				
11		17	43	>300
24		41	27	32
19		0.0006	4.8	>160

for the other enzymes analyzed as evidenced by comparing the  $K_i$  values of the headgroup **11** with that of compound **24** (Table 3). This observation fully agrees with our previous experiences with  $\beta$ -cyclodextrin as carrier of diverse other ligands [28–30].

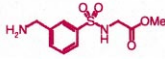
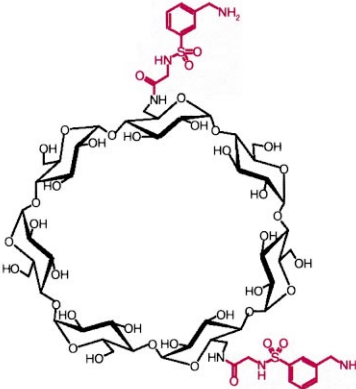
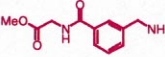
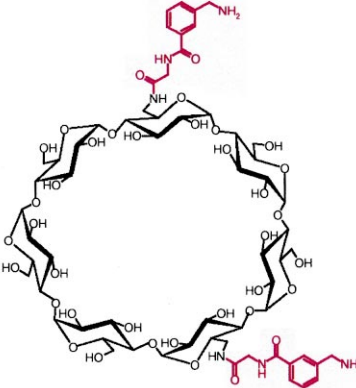
The replacement of the freely rotatable sulfonamide bond in compound **19** with the planar carboxamide bond in construct **30** most surprisingly produced a dramatic reduction of affinity for tryptase. In fact, comparing its binding affinity to that of the headgroup 3-(aminomethyl)benzoyl as glycine methyl ester (**26**) ( $K_i$  0.4 and 74  $\mu$ M, respectively), only a 160-fold increased inhibitory potency was determined for the bivalent construct (Table 4). This suggests that the limitation of the free rotation of the headgroup prevents optimal occupation of the two S1 subsites, most probably due to a penalty caused by enthalpic strains.

## 2.6. Bivalent binding of the $\beta$ -cyclodextrin inhibitor **19** to $\beta$ -tryptase

The strong influence of the type and size of the spacer between the carbohydrate template and the headgroups on binding affinities and the absence of contributions to binding by the cyclodextrin moiety per se fully support a bivalent binding mode of the inhibitor **19** to two adjacent active sites of the  $\beta$ -tryptase tetramer. Correspondingly, the expected stoichiometry for inactivation of the A/D and B/C pairs of active sites is 2:1 for inhibitor **19**/tetrameric enzyme. Titration of  $\beta$ -tryptase with compound **19** yields a ratio of  $1.93 \pm 0.1$ , which fully agrees with the theoretical one (Fig. 3). Further evidence for the bivalent binding mode could be derived from X-ray structure analysis of  $\beta$ -tryptase/inhibitor **19** crystals. Despite the low resolution (3.2 Å), the  $2F_{\text{obs}} - F_{\text{calc}}$  density map clearly

Table 4

Inhibition of the  $\beta$ -tryptase tetramer by  $\beta$ -cyclodextrin-based bivalent inhibitors: influence of the replacement of the sulfonyl group by a carbonyl group on the inhibitory potency

Compound	Structure	$K_i$ [ $\mu$ M]
11		17
19		0.0006
26		74
30		0.4

reveals well defined positions of two cyclodextrin moieties between the A/D and B/C active sites, respectively, in correct distance for occupancy of the S1 subsites by the identical headgroups (Fig. 4). The depicted model of the inhibitor **19** serves only to illustrate that the position of the cyclodextrin moiety allows binding of the headgroups into the specificity pockets. At the present state of refinement, the electron density does not allow us to localize the atom positions of the two identical side chains exactly. The detailed structural analysis will be reported elsewhere.

#### 2.7. Structural stabilization of the tetrameric $\beta$ -tryptase with inhibitors

As shown by the X-ray structure, large contact areas

between the subunits A/D and B/C ( $1075 \text{ \AA}^2$  each) together with stabilizing hydrophobic contacts, salt bridges, and hydrogen bonds involving both main and side chains (Fig. 1) are responsible for the tight assembly of these monomers [23,24]. The contact areas between the subunits A/B and C/D are significantly smaller ( $540 \text{ \AA}^2$ ), and these interfaces are exclusively hydrophobic in nature. Most likely, the known tetramer stabilizing effect of high salt concentrations [33,34] is due to the strengthening of these hydrophobic interactions and weakening of the arginine/arginine repulsion within these interfaces. In vivo,  $\beta$ -tryptase is secreted by mast cells as a tetramer stabilized by heparin proteoglycans [35,36], which are thought to bind to clusters of positively charged residues on both sides of the A/B and C/D interface. In the absence of stabilizing

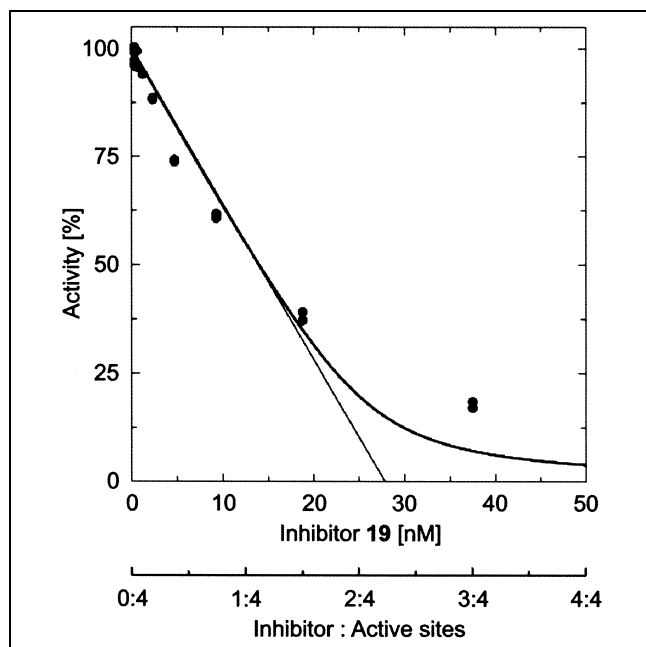


Fig. 3. Titration of  $\beta$ -tryptase (12.5 nM tetramer, i.e. 50 nM active sites) with the bivalent inhibitor **19**.

glycosaminoglycans or high salt concentrations, the enzymatically active tetramer rapidly dissociates into the monomers which are virtually inactive [33,34,37,38]. In the enzymatically active tetramer, the N-terminal Ile-16 residue of each monomer is inserted into the Ile-16 pocket and forms a solvent-inaccessible salt bridge between its  $\alpha$ -amino group and the side chain carboxylate of Asp-194. This salt bridge is found in virtually all mature trypsin-like proteases and is required for the formation of the functional substrate recognition subsites [39,40]. This rearrangement of the active site leads to local alterations of the environment of a tryptophan residue and thus to a significantly altered dichroic contribution in the far-UV

circular dichroism (CD) spectrum that produces a negative maximum centered at 230 nm. For chymotrypsin this role was assigned to Trp-141 [41], but Trp-215 has also been proposed as the responsible residue [42]. The CD spectra of tryptases from various organisms are also characterized by this negative dichroic peak at 230 nm, which according to the amino acid sequence alignment [43,23] could originate from Trp-130 (tryptase numbering). Upon inactivation of tryptase, this characteristic dichroic minimum disappears [44,45], thus making it possible to monitor by CD a conversion of tetrameric tryptase into monomers.

Heat denaturation of  $\beta$ -tryptase in the absence of the stabilizing heparin and at physiological salt concentration (150 mM) exhibits a two-phase transition (Fig. 5). In agreement with similar studies reported previously [44], the first transition is characterized by a decrease of the dichroic intensity at 230 nm and corresponds to the dissociation of the tetramer into monomers and thus parallels the loss of enzymatic activity. It is followed by a second transition ( $T_m = 62.4^\circ\text{C}$ ), which results from thermal denaturation of the monomers as assessed by monitoring thermal unfolding of the monomer at 215 nm (data not shown). Addition of the monovalent inhibitor **11** at concentrations sufficient to occupy all four active sites led to a remarkable stabilization of the tetramer ( $T_m = 48.3^\circ\text{C}$ ). A stabilizing effect of the peptide aldehyde leupeptin on tryptase against time-dependent spontaneous inactivation has been reported previously [45]. Cross-bridging of the A/D and B/C monomers by the bivalent inhibitor **19** results in a weak, but well detectable increase of the  $T_m$  value to  $49.9^\circ\text{C}$ .

### 3. Discussion

From theoretical considerations on polyvalent binding

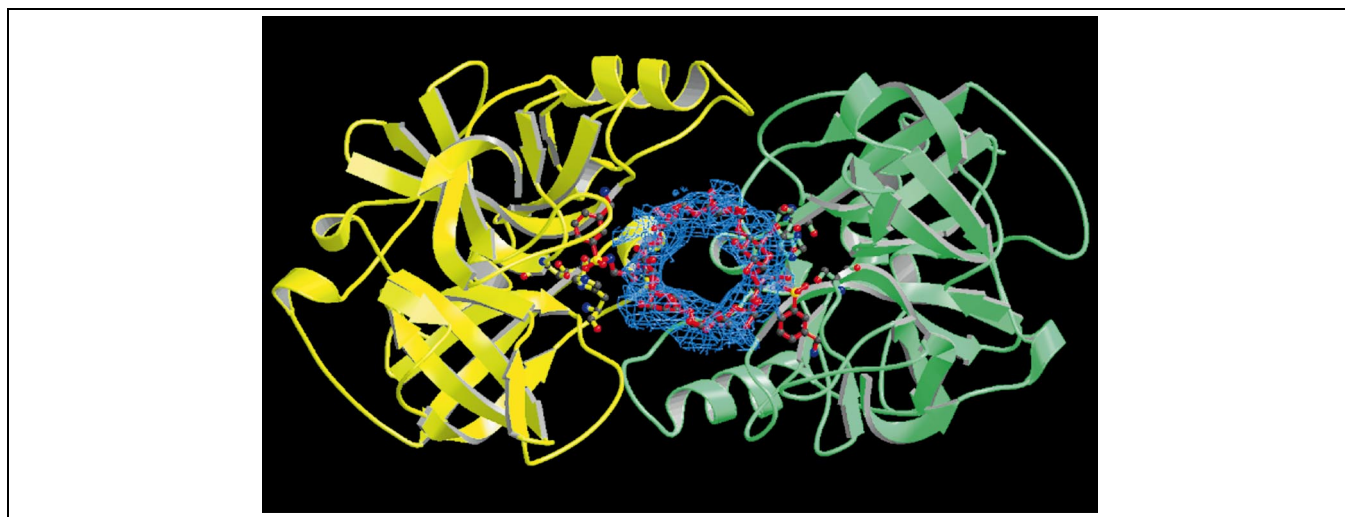


Fig. 4. X-ray structure of the  $\beta$ -tryptase tetramer in complex with the bivalent inhibitor **19**. The tryptase subunits A (green) and D (yellow) are shown in ribbon representation with the amino acid residues of the catalytic triad (Ser-195, His-57, and Asp-102) as stick and ball models. The inhibitor **19** is shown in stick and ball representation, sticks are colored red, C atoms black, O atoms red, N atoms blue, and S atoms yellow.

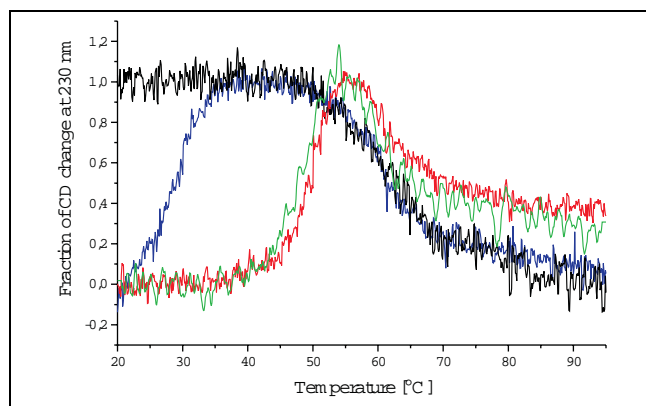


Fig. 5. Thermal denaturation of the  $\beta$ -tryptase tetramer and monomer without stabilizing heparin at low salt conditions (150 mM NaCl). Blue:  $\beta$ -tryptase tetramer without inhibitor; black:  $\beta$ -tryptase monomer; green:  $\beta$ -tryptase tetramer in the presence of 1 mM **11**; red:  $\beta$ -tryptase tetramer in the presence of 10  $\mu$ M **19**.

of ligands to receptor molecules, thermodynamic correlations were derived which were validated experimentally by Whitesides and coworkers [19,20] with the classical study of the vancomycin system. The thermodynamics of monovalent and bivalent inhibition of the  $\beta$ -tryptase tetramer are outlined in Fig. 6. Ideally, the enthalpy of binding of a bivalent inhibitor into two identical active sites should correspond to two times that of the monomer, while the loss of entropy, in such a case dominated by translational entropy, should be approximately that of the monomer. Such ideal bivalent inhibitors require a rigid template that allows the headgroups to interact with the enzyme binding subsites without enthalpic strains and with a minimal loss of conformational entropy. Conversely, for flexible ligands a high penalty from the conformational entropy can largely offset the favorable translational and rotational entropy term.

In view of these thermodynamic aspects, the low gain in binding affinity obtained with the bivalent PEG-based inhibitor **3** has to be attributed mainly to its high degree of flexibility. Although the flexible PEG spacer allows for binding of the headgroups to the active sites without enthalpic strains, the large penalty resulting from the loss of conformational entropy makes binding at the second site energetically less favored. Similar low gains in binding energies have previously been reported for the use of PEG as spacer of bidentate ligands [6,9]. In the case of the proteasome where diffusion into and out of the catalytic chamber is hampered by the bottleneck of the cylindrical structure, bivalent binding of such PEG-based inhibitors is apparently more favored by their seclusion in the digestion chamber [25], whereas in the case of the tryptase tetramer diffusion into the bulk solvent from the central pore is not hindered at all.

In the  $\beta$ -cyclodextrin construct **19** only the four bonds related to the glycine spacer allow for free rotational motions and thus for optimal occupancy of the S1 binding pockets. Upon binding, these bonds are probably frozen

into a defined conformation, but the related loss of conformational entropy is insufficient to compensate for the gains in the translational and rotational entropy term. Correspondingly, the free energies of binding of the bivalent inhibitor become additive with the  $K_{i,bi} \approx (K_{i,mono})^2$  and a cooperativity factor [1]  $\alpha = (\log K_{i,bi})/(\log K_{i,mono})$  of 1.9 versus the theoretical value of 2. This result fully

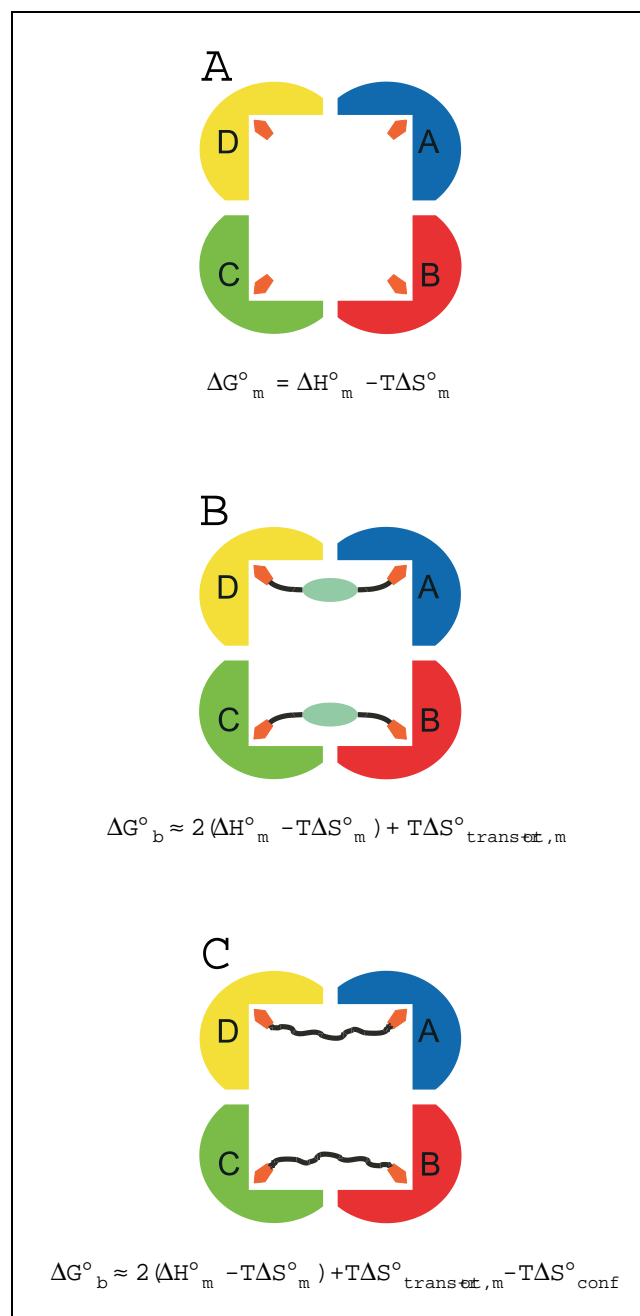


Fig. 6. Thermodynamics of the inhibition of  $\beta$ -tryptase by mono- and bivalent inhibitors. (A) Binding head. (B) Bivalent inhibitor with perfectly fitting, rigid spacer. (C) Bivalent inhibitor with flexible spacer.  $\Delta G^\circ_m$ ,  $\Delta H^\circ_m$  and  $T\Delta S^\circ_m$  are the free energy, enthalpy, and entropy of monovalent inhibition, respectively;  $T\Delta S^\circ_{trans+rot,m}$  is the translational and rotational entropy of monovalent inhibition;  $\Delta G^\circ_b$  is the free energy of bivalent inhibition, and  $T\Delta S^\circ_{conf}$  is the loss of conformational entropy in the two intramolecular binding events.

confirms the advantage of rigid scaffolds for the design of homobivalent inhibitors. However, it also reveals the limits that are derived from the need of optimal fitting of both heads, as small deviations lead to significant losses of binding affinity. In fact, a slight increase in the size of the spacer, i.e. the replacement of the glycine residue with  $\beta$ -alanine, already affects the inhibitory potency. More dramatic was the effect of replacing the sulfonamide bond with a carboxamide bond as the bivalent effect was almost fully lost. The resulting potentiation of binding affinity of the dibasic compound **30** ( $K_i = 0.4 \mu\text{M}$  versus  $K_i = 74 \mu\text{M}$  of the headgroup **26**) does not necessarily result from a homobivalent binding as it could well derive from exosite binding of the second basic group. This is supported by results of X-ray analysis of supposedly homobivalent dibasic trypsin inhibitors, which were found to interact with the second basic group at exosites (unpublished results).

#### 4. Significance

The main advantage of the design of bivalent inhibitors of multicatalytic protease complexes such as the tetrameric  $\beta$ -trypsin is certainly the high degree of selectivity that can be obtained. In fact, the potentiation of binding affinity of weakly binding headgroups with poor affinity for other monomeric enzymes can be exploited by this approach to produce highly specific inhibitors. Because there are strong indications from an increasing number of studies that trypsin is directly involved in the pathogenesis of asthma [46–51], the tetrameric architecture of this trypsin-like serine protease has already been successfully exploited for the design of dibasic inhibitors. Without knowledge of the exact structure of the tetramer, some of the dibasic compounds were too small for bivalent inhibition [52,53], whereas screening with more or less flexible spacers of increasing length led to highly potent inhibitors [49,54–57]. However, potentiation of binding affinities of dibasic compounds does not necessarily result only from a more or less optimal homobivalent binding, but could also derive from less defined exosite interactions.

#### 5. Experimental procedures

##### 5.1. Materials and methods

All reagents and solvents used in the synthesis were of the highest quality commercially available.  $\beta$ -Cyclodextrin was purchased from Fluka, biphenyl-4,4'-disulfonyl chloride and 3-cyanobenzoyl chloride from Aldrich, 3-cyanobenzenesulfonyl chloride from Maybridge Chemical Company, and the ion exchange resin Serdolite MB-3 from Serva. Thin layer chromatography (TLC) was carried out on silica gel 60 plates (Merck AG, Darmstadt) and compounds were visualized by chlorine/o-toluidine and

ninhydrin reagents. Cyclodextrin derivatives were detected by dipping the TLC plates into 5% sulfuric acid in methanol followed by heating. Analytical high performance liquid chromatography (HPLC) was carried out with Waters equipment (Eschborn) on Nucleosil 100-5/C8 (Macherey and Nagel, Düren) using a linear gradient of acetonitrile/2%  $\text{H}_3\text{PO}_4$  from 5:95 to 80:20 in 12 min, preparative HPLC on Nucleosil 100-5/C18 (Macherey and Nagel, Düren) using a linear gradient of 0.1% aqueous TFA/acetonitrile from 98:2 to 68:32 in 30 min. The product content of the inhibitors with the exception of **8** was determined by quantitative amino acid analysis of the acid hydrolysates (6 M HCl; 110°C; 48 h) performed on a Biotronic amino acid analyzer (LC 6001). Electrospray ionization mass spectrometry (ESI-MS) spectra were recorded on PE SCIEX API 165.

##### 5.2. Synthesis

The tripeptide aldehyde Ac-Arg-Val-Arg-H (**1**) and the related PEG conjugates **2** and **3** were prepared as described previously [26].

##### 5.2.1. 6A,6D-Diazido-6A,6D-dideoxy- $\beta$ -cyclodextrin (**5**)

To a solution of biphenyl-4,4'-disulfonyl-*A,D*-capped  $\beta$ -cyclodextrin (**4**) [30] (1.40 g, 0.99 mmol) in DMF (20 ml)  $\text{NaN}_3$  (0.52 g, 7.92 mmol) was added, and the stirred reaction mixture was kept for 24 h at 70°C. The solvent was evaporated and the residue dissolved in water. Upon addition of Serdolite MB-3 until a pH of approximately 5 was reached, the ion exchange resin was filtered off, the water evaporated and the residue reevaporated from toluene ( $3\times$ ). The white powder was suspended in acetone, filtered off, washed successively with acetone, *tert*-butyl methyl ether and petroleum ether, and dried at 40°C in vacuo; yield: 1.10 g (94%); TLC (isopropanol/AcOEt/ $\text{NH}_3/\text{H}_2\text{O}$ , 7:7:5:4)  $R_f$  0.4; ESI-MS:  $m/z$  1185.4  $[\text{M}+\text{H}]^+$ ; calcd. for  $\text{C}_{42}\text{H}_{68}\text{N}_6\text{O}_{33}$ : 1184.4.

##### 5.2.2. 6A,6D-Diamino-6A,6D-dideoxy- $\beta$ -cyclodextrin (**6**)

To a stirred solution of **5** (0.475 g, 0.40 mmol) in DMF (10 ml),  $\text{PPh}_3$  (0.629 g, 2.40 mmol) was added. After 1.5 h, 25% aqueous ammonia (5 ml) was added and the reaction mixture was stirred overnight. The solvent was evaporated, the residue was taken up with water and the insoluble  $\text{PPh}_3$  oxide was filtered off and the filtrate evaporated. The product was isolated as white powder by precipitation from water/acetone; yield: 0.41 g (91%); TLC (isopropanol/AcOEt/ $\text{NH}_3/\text{H}_2\text{O}$ , 7:7:5:4)  $R_f$  0.25; ESI-MS:  $m/z$  1133.6  $[\text{M}+\text{H}]^+$ ; calcd. for  $\text{C}_{42}\text{H}_{72}\text{N}_2\text{O}_{33}$ : 1132.4.

##### 5.2.3. 6A,6D-Bis(3-cyanobenzenesulfonyl-amino)-6A,6D-dideoxy- $\beta$ -cyclodextrin (**7**)

To a stirred solution of **6** (100.0 mg, 0.088 mmol) 0.1 N NaOH (1.76 ml) followed by 3-cyanobenzenesulfonyl chloride (1.76 ml of a solution ( $c = 0.1 \text{ mol/l}$ ) in acetonitrile) was added. After 30 min again 0.1 N NaOH (0.35 ml) and 3-cyanobenzenesulfonyl chloride (0.35 ml) was added, and stirring was continued for an additional 2 h. Then the solution was treated with Serdolite MB-3 for 3 h, the ion exchange resin was filtered off, and the solvent

was evaporated. The material obtained was suspended in acetone, collected by centrifugation, washed successively with acetone, *tert*-butyl methyl ether and petroleum ether, and dried at 40°C in vacuo; yield: 70 mg (54%); HPLC  $t_R$  7.4 min; ESI-MS:  $m/z$  1463.6  $[M+H]^+$ ; calcd. for  $C_{56}H_{78}N_4O_{37}S_2$ : 1462.4.

#### 5.2.4. 6*A*,6*D*-Bis[3-(aminomethyl)benzenesulfonylamino]-6*A*,6*D*-dideoxy- $\beta$ -cyclodextrin (**8**)

**7** (60.0 mg, 0.041 mmol) in 90% AcOH (180 ml) was hydrogenated over 10% Pd-C at atmospheric pressure. After 24 h the solvent was removed in vacuo and the residual oil was evaporated from toluene (3 $\times$ ). The crude product was purified by preparative HPLC and the homogeneous fractions were collected and lyophilized. The product was obtained as bistrifluoroacetate; yield: 26 mg (37%); HPLC  $t_R$  6.0 min; ESI-MS:  $m/z$  736.4  $[M+2H]^{2+}$ ; calcd. for  $C_{56}H_{86}N_4O_{37}S_2$ : 1470.4.

#### 5.2.5. 3-(Aminomethyl)benzenesulfonyl-glycine methyl ester (**11**)

3-Cyanobenzenesulfonyl-glycine methyl ester (**9**) (0.80 g, 3.14 mmol; prepared by standard procedures from 3-cyanobenzenesulfonyl chloride and glycine methyl ester) was hydrogenated over 10% Pd-C at atmospheric pressure in AcOH (75 ml). The reduction was completed within 5 h (TLC control) and the catalyst was filtered off. The filtrate was concentrated and the resulting oil was evaporated from toluene (3 $\times$ ). The title compound was isolated in the acetate form as a white powder by precipitation from MeOH/*tert*-butyl methyl ether; yield: 0.76 g (76%); TLC (*n*-butanol/AcOH/H<sub>2</sub>O/AcOEt, 3:1:1:5)  $R_f$  0.15; product content: 60.9%; ESI-MS:  $m/z$  259.0  $[M+H]^+$ ; calcd. for  $C_{10}H_{14}N_2O_4S$ : 258.0.

#### 5.2.6. 3-(Aminomethyl)benzenesulfonyl- $\beta$ -alanine methyl ester (**12**)

3-Cyanobenzenesulfonyl- $\beta$ -alanine methyl ester (**10**) (obtained by standard procedures from 3-cyanobenzenesulfonyl chloride and  $\beta$ -alanine methyl ester) was hydrogenated as described for **11**. The product was isolated in the acetate form; yield: 74%; TLC (*n*-butanol/AcOH/H<sub>2</sub>O/AcOEt, 3:1:1:5)  $R_f$  0.2; ESI-MS:  $m/z$  273.2  $[M+H]^+$ ; calcd. for  $C_{11}H_{16}N_2O_4S$ : 272.0.

#### 5.2.7. 3-(*tert*-Butoxycarbonylaminoethyl)benzenesulfonyl glycine (**15**)

To a stirred solution of **11** (0.60 g, 1.88 mmol) in dioxane/H<sub>2</sub>O (1:1, 30 ml), NaHCO<sub>3</sub> (0.158 g, 1.88 mmol) followed by (Boc)<sub>2</sub>O (0.451 g, 2.07 mmol) was added. After 1 h, an additional portion of (Boc)<sub>2</sub>O (0.205 g, 0.94 mmol) was added and the solution stirred for a further 30 min. Then the solvent was evaporated to dryness; the resulting oil was dissolved in THF (30 ml) and 0.1 N NaOH (19 ml) was added dropwise. After 24 h, the solvent was evaporated, the residual oil dissolved in water (100 ml) and washed with AcOEt (3 $\times$  50 ml). The aqueous phase was acidified with 5% aq KHSO<sub>4</sub> and extracted with AcOEt (3 $\times$  50 ml), the combined organic layers were washed with brine (30 ml) and dried (Na<sub>2</sub>SO<sub>4</sub>). The solvent was evaporated and the product was isolated by precipitation from AcOEt/petroleum ether as a

colorless powder; yield: 0.45 g (70%); TLC (*n*-butanol/AcOH/H<sub>2</sub>O/AcOEt, 3:1:1:5)  $R_f$  0.8; ESI-MS:  $m/z$  367.2  $[M+Na]^+$ ; calcd. for  $C_{14}H_{20}N_2O_6S$ : 344.1.

#### 5.2.8. 3-(*tert*-Butoxycarbonylaminoethyl)benzenesulfonyl- $\beta$ -alanine (**16**)

The title compound was obtained from **12** as described for **15**; yield: 76%; TLC (cyclohexane/CHCl<sub>3</sub>/AcOH, 45:45:10)  $R_f$  0.1; ESI-MS:  $m/z$  359.0  $[M+H]^+$ ; calcd. for  $C_{15}H_{22}N_2O_6S$ : 358.1.

#### 5.2.9. 6*A*,6*D*-Bis[3-(*tert*-butoxycarbonylaminoethyl)benzenesulfonyl-glycyl-amino]-6*A*,6*D*-dideoxy- $\beta$ -cyclodextrin (**17**)

To a stirred solution of **6** (100.0 mg, 0.088 mmol), **15** (72.9 mg, 0.211 mmol), and PyBOP (110.2 mg, 0.211 mmol) in DMF (7.5 ml), DIEA (36.5  $\mu$ l, 0.211 mmol) was added. After 24 h, the solvent was evaporated and the oily residue treated with acetone. The colorless precipitate was collected by centrifugation, washed successively with acetone, *tert*-butylmethyl ether, and petroleum ether and dried at 40°C in vacuo; yield: 105.0 mg (67%); HPLC:  $t_R$  6.7 min; ESI-MS:  $m/z$  1786.8  $[M+H]^+$ ; calcd. for  $C_{70}H_{108}N_6O_{43}S_2$ : 1784.6.

#### 5.2.10. 6*A*,6*D*-Bis[3-(*tert*-butoxycarbonylaminoethyl)benzenesulfonyl- $\beta$ -alanyl-amino]-6*A*,6*D*-dideoxy- $\beta$ -cyclodextrin (**18**)

The title compound was obtained from **6** and **16** as described for **17**; yield: 71%; HPLC:  $t_R$  8.3 min; ESI-MS:  $m/z$  1815.2  $[M+H]^+$ ; calcd. for  $C_{72}H_{112}N_6O_{43}S_2$ : 1812.6.

#### 5.2.11. 6*A*,6*D*-Bis[3-(aminomethyl)benzenesulfonyl-glycyl-amino]-6*A*,6*D*-dideoxy- $\beta$ -cyclodextrin (**19**)

**17** (100.0 mg, 0.055 mmol) was dissolved in ice-cold 90% TFA (10 ml). After 3 h, the acid was removed in vacuo and the residual oil was evaporated from toluene (3 $\times$ ). The title compound was isolated as bistrifluoroacetate by precipitation from water/acetone; yield: 85.0 mg (85%); HPLC  $t_R$  4.0 min; product content: 32.0%; ESI-MS:  $m/z$  793.4  $[M+2H]^{2+}$ ; calcd. for  $C_{60}H_{92}N_6O_{39}S_2$ : 1584.5.

#### 5.2.12. 6*A*,6*D*-Bis[3-(aminomethyl)benzenesulfonyl- $\beta$ -alanyl-amino]-6*A*,6*D*-dideoxy- $\beta$ -cyclodextrin (**20**)

The title compound was obtained from **18** as bistrifluoroacetate as described for **19**; yield: 52%; HPLC  $t_R$  2.6 min; product content: 31.1%; ESI-MS:  $m/z$  807.4  $[M+2H]^{2+}$ ; calcd. for  $C_{62}H_{96}N_6O_{39}S_2$ : 1612.5.

#### 5.2.13. Mono-{2,3-di-*O*-acetyl-6-[3-(*tert*-butoxycarbonylaminoethyl)benzenesulfonyl-glycyl-amino]-6-deoxy}-hexakis-(2,3,6-tri-*O*-acetyl)- $\beta$ -cyclodextrin (**22**)

To a stirred solution of mono-(2,3-di-*O*-acetyl-6-amino-6-deoxy)-hexakis-(2,3,6-tri-*O*-acetyl)- $\beta$ -cyclodextrin (**21**) [27] (100.0 mg, 0.050 mmol), **15** (20.9 mg, 0.060 mmol), and HOBt (8.2 mg, 0.060 mmol) in CHCl<sub>3</sub> (5 ml), EDC (11.6 mg, 0.060 mmol) was added. After 24 h, the solvent was evaporated and the crude residue was purified on a silica gel column (3 $\times$  7 cm) using tol-

uene/EtOH (2:1) as eluent. Evaporation of the solvent furnished a white solid; yield: 106.0 mg (92%); TLC (toluene/EtOH, 2:1)  $R_f$  0.7; ESI-MS:  $m/z$  2318.8  $[M+H_2O+H]^+$ ; calcd. for  $C_{96}H_{129}N_3O_{59}S$ : 2299.7.

**5.2.14. 6-[3-(*tert*-Butoxycarbonylaminoethyl)benzenesulfonyl-glycyl-amino]-6-deoxy- $\beta$ -cyclodextrin (**23**)**

To a stirred solution of **22** (106 mg, 0.046 mmol) in MeOH (10 ml) 0.1 N NaOH (1.10 ml) was added. The precipitate which had been formed after a short period was dissolved by adding water. After 4 h, Serdolit MB-3 was added. After the pH had reached a value of about 5, the ion exchange resin was filtered off and the solvent was evaporated. The title compound was isolated by precipitation from water/acetone; yield: 57 mg (85%); HPLC  $t_R$  5.9 min; ESI-MS:  $m/z$  1460.6  $[M+H]^+$ ; calcd. for  $C_{56}H_{89}N_3O_{39}S$ : 1459.5.

**5.2.15. 6-[3-(Aminomethyl)benzenesulfonyl-glycylamino]-6-deoxy- $\beta$ -cyclodextrin (**24**)**

The acidolytic cleavage of the *tert*-butoxycarbonyl (Boc) group from **23** was performed as described for **19**. The product was isolated as trifluoroacetate; yield: 59 mg (quant.); HPLC  $t_R$  4.3 min; product content: 45.3%; ESI-MS:  $m/z$  1360.6  $[M+H]^+$ ; calcd. for  $C_{51}H_{81}N_3O_{37}S$ : 1359.4.

**5.2.16. 3-(Aminomethyl)benzoyl-glycine methyl ester (**26**)**

3-Cyanobenzoyl-glycine methyl ester (**25**) (obtained by standard procedures from 3-cyanobenzoyl chloride and glycine methyl ester) was hydrogenated as described for **11** and isolated as hydrochloride; yield: 66%; TLC (CHCl<sub>3</sub>/MeOH/AcOH, 8:8:1)  $R_f$  0.4; product content: 90.3%; ESI-MS:  $m/z$  223.0  $[M+H]^+$ ; calcd. for  $C_{11}H_{14}N_2O_3$ : 222.1.

**5.2.17. 3-(*tert*-Butoxycarbonylaminoethyl)benzoyl-glycine (**28**)**

The title compound was obtained from **26** as described for **15**; yield: 71%; TLC (*n*-butanol/AcOH/H<sub>2</sub>O/AcOEt, 3:1:1:5)  $R_f$  0.8; ESI-MS:  $m/z$  309.2  $[M+H]^+$ ; calcd. for  $C_{15}H_{20}N_2O_5$ : 308.1.

**5.2.18. 6A,6D-Bis[3-(*tert*-butoxycarbonylaminoethyl)benzoyl-glycyl-amino]-6A,6D-dideoxy- $\beta$ -cyclodextrin (**29**)**

The title compound was obtained from **6** and **28** as described for **17**; yield: 72%; HPLC  $t_R$  8.0 min; ESI-MS:  $m/z$  1714.0  $[M+H]^+$ ; calcd. for  $C_{72}H_{108}N_6O_{41}$ : 1712.6.

**5.2.19. 6A,6D-Bis[3-(aminomethyl)benzoyl-glycyl-amino]-6A,6D-dideoxy- $\beta$ -cyclodextrin (**30**)**

The title compound was obtained from **29** as bistrifluoroacetate as described for **19**; yield: 94%; HPLC  $t_R$  5.6 min; product content: 81.6%; ESI-MS:  $m/z$  757.4  $[M+2H]^{2+}$ ; calcd. for  $C_{62}H_{92}N_6O_{37}$ : 1512.5.

**5.3. Kinetic measurements**

Equilibrium dissociation constants ( $K_i$ ) for the complexes of the inhibitors with tryptase, thrombin, and trypsin were deter-

mined essentially as described previously [58]. Briefly, human  $\beta$ -tryptase isolated from lung tissue or produced recombinantly, human thrombin, and bovine pancreatic trypsin were standardized by active site titration using 4-methylumbelliferyl *p*-guanidinobenzoate. A constant concentration of an enzyme (0.1–1 nM;  $[E] < K_i$ ) was incubated with increasing concentrations of an inhibitor for 1 h. Subsequently the residual enzyme activity was measured by following the hydrolysis of a fluorogenic substrate in a Biolumin 960 microplate reader (Amersham). Apparent  $K_i$  values were obtained by fitting the steady-state velocities to the equation for tight-binding inhibitors [59] using non-linear regression analysis, and  $K_i$  values calculated by correction for the competition between inhibitor and substrate. Similarly, the stoichiometry of the interaction of inhibitor **19** with the tryptase tetramer was determined; however, an active site concentration of 50 nM ( $[E]/K_i \approx 80$ ) was used.

**5.4. CD measurements**

The CD spectra were recorded on a Jasco spectropolarimeter J-715 equipped with a temperature-controlled cell holder (Model PFD-350S) using a quartz cell with a path length of 0.1 cm. For thermal denaturation a heating rate of 30°C/h was applied. Solutions of  $\beta$ -tryptase as tetramer (6.7  $\mu$ M) and monomer (26.8  $\mu$ M) were prepared in 50 mM Tris-HCl buffer containing 150 mM NaCl (pH 7.6) and concentrations of the bivalent inhibitor **19** (10  $\mu$ M) and monovalent inhibitor **11** (1 mM) to ascertain virtually full occupancy of the S1 subsites.

**5.5. X-ray analysis**

The successful crystallization of previously inhibited and recombinant  $\beta$ -tryptase at room temperature using vapor diffusion methods will be published elsewhere. Initial small crystals of almost cubic shape were grown within a week and used for macroseeding. The final crystals, 100  $\times$  100  $\times$  80  $\mu$ m in size, suffered from radiation damage such that cryo conditions were required. Data collection was performed at 100 K at the wiggler beamline BW6 at DORIS (Deutsches Elektronensynchrotron, Hamburg) using a CCD detector (Mar Research, Hamburg), a Cryostream cryosystem (Oxford Cryosystems, Oxford) and flash-frozen crystals. The data were measured in frames of 0.8° through a continuous angular range of 180°. The crystal belonged to space group P1 with unit cell dimensions of  $a = 107.35$  Å,  $b = 107.91$  Å,  $c = 109.04$  Å,  $\alpha = 89.92^\circ$ ,  $\beta = 89.44^\circ$ ,  $\gamma = 120.36^\circ$ . Freezing caused slight disorder within the crystal lattice, resulting in a low completeness of 87.3%. The current crystallographic *R* factor is 31% ( $R_{free} = 37\%$ ).

**Acknowledgements**

The study was supported by SFB 469 of the Ludwig-Maximilians-University of München and by Byk-Gulden, Konstanz, Germany with postdoc/doctoral grants for N.S., A.B., and U.M.

## References

- [1] M. Mammen, S.-K. Choi, G.M. Whitesides, Polyvalent interactions in biological systems – Implications for design and use of multivalent ligands and inhibitors, *Angew. Chem. Int. Ed. Engl.* 37 (1998) 2755–2794.
- [2] L.L. Kiessling, N.L. Pohl, Strength in numbers: non-natural polyvalent carbohydrate derivatives, *Chem. Biol.* 3 (1996) 71–77.
- [3] Y.C. Lee, R.T. Lee, Carbohydrate-protein interactions: basis of glycobiology, *Acc. Chem. Res.* 28 (1995) 321–327.
- [4] M.N. Matrosovich, Towards the development of antimicrobial drugs acting by inhibition of pathogen attachment to host cells: a need for polyvalency, *FEBS Lett.* 252 (1989) 1–4.
- [5] A. Spaltenstein, G.M. Whitesides, Polyacrylamides bearing pendant  $\alpha$ -sialoside groups strongly inhibit agglutination of erythrocytes by influenza virus, *J. Am. Chem. Soc.* 113 (1991) 686–687.
- [6] G.D. Glick, P.L. Toogood, D.C. Wiley, J.J. Skehel, J.R. Knowles, Ligand recognition by influenza virus. The binding of bivalent sialosides, *J. Biol. Chem.* 266 (1991) 23660–23669.
- [7] E. Fan, Z. Zhang, W.E. Minke, Z. Hou, C.L.M.J. Verlinde, W.G.J. Hol, High-affinity pentavalent ligands of *Escherichia coli* heat-labile enterotoxin by modular structure-based design, *J. Am. Chem. Soc.* 122 (2000) 2663–2664.
- [8] M.G. Carrithers, M.R. Lerner, Synthesis and characterization of bivalent peptide ligands targeted to G-protein-coupled receptors, *Chem. Biol.* 3 (1996) 537–542.
- [9] R.H. Kramer, J.W. Karpen, Spanning binding sites on allosteric proteins by polymer-linked ligand dimers, *Nature* 395 (1998) 710–713.
- [10] J.C. Cheronis, E.T. Whalley, K.T. Nguyen, S.R. Eubanks, L.G. Allen, M.J. Duggan, S.D. Loy, K.A. Bonham, J.K. Blodgett, A new class of bradykinin antagonists: synthesis and in vitro activity of bis-succinimidoalkane peptide dimers, *J. Med. Chem.* 35 (1992) 1563–1572.
- [11] Y.-P. Pang, P. Quiram, T. Jelacic, F. Hong, S. Brimijoin, Highly potent, selective, and low cost bis-tetrahydroaminacrine inhibitors of acetylcholinesterase. Steps toward novel drugs for treating Alzheimer's disease, *J. Biol. Chem.* 271 (1996) 23646–23649.
- [12] A.A. Profit, T.R. Lee, D.S. Lawrence, Bivalent inhibitors of protein tyrosine kinases, *J. Am. Chem. Soc.* 121 (1999) 280–283.
- [13] J. Dodt, Anticoagulatory substances of bloodsucking animals – from hirudin to hirudin mimetics, *Angew. Chem. Int. Ed. Engl.* 34 (1995) 867–880.
- [14] T. Steinmetzer, B.Y. Zhu, Y. Konishi, Potent bivalent thrombin inhibitors: replacement of the scissile peptide bond at P<sub>1</sub>–P<sub>1</sub>' with arginyl ketomethylene isosteres, *J. Med. Chem.* 42 (1999) 3109–3115.
- [15] T. Steinmetzer, M. Renatus, S. Kunzel, A. Eichinger, W. Bode, P. Wikstrom, J. Hauptmann, J. Stürzebecher, Design and evaluation of novel bivalent thrombin inhibitors based on amidinophenylalanines, *Eur. J. Biochem.* 265 (1999) 598–605.
- [16] D.M. Crothers, H. Metzger, The influence of polyvalency on the binding properties of antibodies, *Immunochemistry* 9 (1972) 341–357.
- [17] H.P. Rappaport, Evaluation of group contributions to ligand binding, *J. Theor. Biol.* 79 (1979) 157–165.
- [18] W.P. Jencks, On the attribution and additivity of binding energies, *Proc. Natl. Acad. Sci. USA* 78 (1981) 4046–4050.
- [19] J. Rao, J. Lahiri, L. Isaacs, R.M. Weis, G.M. Whitesides, A trivalent system from vancomycin-D-Ala-D-Ala with higher affinity than avidin-biotin, *Science* 280 (1998) 708–711.
- [20] J. Rao, J. Lahiri, R.M. Weis, G.M. Whitesides, Design, synthesis, and characterization of a high-affinity trivalent system derived from vancomycin and L-Lys-D-Ala-D-Ala, *J. Am. Chem. Soc.* 122 (2000) 2698–2710.
- [21] T.J. Rydel, K.G. Ravichandran, A. Tulinsky, W. Bode, R. Huber, C. Roitsch, J.W. Fenton II, The structure of a complex of recombinant hirudin and human alpha-thrombin, *Science* 249 (1990) 277–280.
- [22] M. Groll, L. Ditzel, J. Löwe, D. Stock, M. Bochtler, H.D. Bartunik, R. Huber, Structure of the 20S proteasome from yeast at 2.4 Å resolution, *Nature* 386 (1997) 463–471.
- [23] P.J. Barbosa Pereira, A. Bergner, S. Macedo-Ribeiro, R. Huber, G. Matschiner, H. Fritz, C.P. Sommerhoff, W. Bode, Human  $\beta$ -tryptase is a ring-like tetramer with active sites facing a central pore, *Nature* 392 (1998) 306–311.
- [24] C.P. Sommerhoff, W. Bode, P.J. Barbosa Pereira, M.T. Stubbs, J. Stürzebecher, G.P. Piechotka, G. Matschiner, A. Bergner, The structure of the human  $\beta$ II-tryptase tetramer: fo(u)r better or worse, *Proc. Natl. Acad. Sci. USA* 96 (1999) 10984–10991.
- [25] G. Loidl, M. Groll, H.-J. Musiol, R. Huber, L. Moroder, Bivalency as a principle for proteasome inhibition, *Proc. Natl. Acad. Sci. USA* 96 (1999) 5418–5422.
- [26] G. Loidl, H.-J. Musiol, M. Groll, R. Huber, L. Moroder, Synthesis of bivalent inhibitors of eucaryotic proteasomes, *J. Peptide Sci.* 6 (2000) 36–46.
- [27] C.P. Sommerhoff, W. Bode, G. Matschiner, A. Bergner, H. Fritz, The human mast cell tryptase tetramer: a fascinating riddle solved by structure, *Biochim. Biophys. Acta* 1477 (2000) 75–89.
- [28] N. Schaschke, H.-J. Musiol, I. Assfalg-Machleidt, W. Machleidt, S. Rudolph-Böhner, L. Moroder, Cyclodextrins as templates for the presentation of protease inhibitors, *FEBS Lett.* 391 (1996) 297–301.
- [29] N. Schaschke, S. Fiori, E. Weyher, C. Escricut, D. Fourmy, G. Müller, L. Moroder, Cyclodextrin as carrier of peptide hormones. Conformational and biological properties of  $\beta$ -cyclodextrin/gastrin constructs, *J. Am. Chem. Soc.* 120 (1998) 7030–7038.
- [30] N. Schaschke, I. Assfalg-Machleidt, W. Machleidt, T. Laibleben, C.P. Sommerhoff, L. Moroder,  $\beta$ -Cyclodextrin/epoxysuccinyl peptide conjugates: a new drug targeting system for tumor cells, *Bioorg. Med. Chem. Lett.* 10 (2000) 677–680.
- [31] I. Tabushi, K. Yamamura, T. Nabeshima, Characterization of regio-specific A,C- and A,D-disulfonate capping of  $\beta$ -cyclodextrin. Capping as an efficient production technique, *J. Am. Chem. Soc.* 106 (1984) 5267–5270.
- [32] J. Coste, D. Le-Nguyen, B. Castro, PyBOP®: a new peptide coupling reagent devoid of toxic by-product, *Tetrahedron Lett.* 31 (1990) 205–208.
- [33] L.B. Schwartz, T.R. Bradford, Regulation of tryptase from human lung mast cells by heparin. Stabilization of the active tetramer, *J. Biol. Chem.* 261 (1986) 7372–7379.
- [34] S.C. Alter, D.D. Metcalf, T.R. Bradford, L.B. Schwartz, Regulation of human mast cell tryptase. Effects of enzyme concentration, ionic strength and the structure and negative charge density of polysaccharides, *Biochem. J.* 248 (1987) 821–827.
- [35] S.M. Goldstein, J. Leong, L.B. Schwartz, D. Cooke, Protease composition of exocytosed human skin mast cell protease-proteoglycan complexes. Tryptase resides in a complex distinct from chymase and carboxypeptidase, *J. Immunol.* 148 (1992) 2475–2482.
- [36] K.A. Lindstedt, J.O. Kokkonen, P.T. Kovanen, Regulation of the activity of secreted human lung mast cell tryptase by mast cell proteoglycans, *Biochim. Biophys. Acta* 1425 (1998) 617–627.
- [37] K.A. Addington, D.A. Johnson, Inactivation of human lung tryptase: evidence for a re-activable tetrameric intermediate and active monomers, *Biochemistry* 35 (1996) 13511–13518.
- [38] A. Kozik, J. Potempa, J. Travis, Spontaneous inactivation of human lung tryptase as probed by size-exclusion chromatography and chemical cross-linking: dissociation of active tetrameric enzyme into inactive monomers is the primary event of the entire process, *Biochim. Biophys. Acta* 1385 (1998) 139–148.
- [39] R. Huber, W. Bode, Structural basis of the activation and action of trypsin, *Acc. Chem. Res.* 11 (1978) 114–122.
- [40] W. Bode, The transition of bovine trypsinogen to a trypsin-like state upon strong ligand binding. II. The binding of the pancreatic trypsin inhibitor and of isoleucine-valine and of sequentially related peptides to trypsinogen and to *p*-guanidinobenzoate-trypsinogen, *J. Mol. Biol.* 127 (1979) 357–374.
- [41] C.R. Cantor, S.N. Timasheff, Optical spectroscopy of proteins, in: H.

- Neurath, R.L. Hill (Eds.), *The Proteins*, 3rd edn., Vol. 5, Academic Press, New York, 1982, pp. 145–306.
- [42] I.B. Grishina, R.W. Woody, Contributions of tryptophan side chains to the circular dichroism of globular proteins: Exciton couplets and coupled oscillators, *Faraday Discuss.* 99 (1994) 245–262.
- [43] D.A. Johnson, G.J. Barton, Mast cell tryptases: examination of unusual characteristics by multiple sequence alignment and molecular modeling, *Protein Sci.* 1 (1992) 370–377.
- [44] L.B. Schwartz, T.R. Bradford, D.C. Lee, J.F. Chlebowski, Immunologic and physicochemical evidence for conformational changes occurring on conversion of human mast cell tryptase from active tetramer to inactive monomer. Production of monoclonal antibodies recognizing active tryptase, *J. Immunol.* 144 (1990) 2304–2311.
- [45] N.M. Schechter, G.Y. Eng, T. Selwood, D.R. McCaslin, Structural changes associated with the spontaneous inactivation of the serine proteinase human tryptase, *Biochemistry* 34 (1995) 10628–10638.
- [46] C.P. Sommerhoff, Dog mast cell proteinases in models of airway secretion, bronchoconstriction, cutaneous vascular permeability, and tissue fibrosis, in: G.H. Caughey (Ed.), *Mast Cell Proteases in Immunology and Biology*, Marcel Dekker, New York, 1995, pp. 145–167.
- [47] G.H. Caughey, Of mites and men – trypsin-like proteases in the lungs, *Am. J. Respir. Cell Mol. Biol.* 16 (1997) 621–628.
- [48] P.R. Johnson, A.J. Ammit, S.M. Carlin, C.L. Armour, G.H. Caughey, J.L. Black, Mast cell tryptase potentiates histamine-induced contraction in human sensitized bronchus, *Eur. Respir. J.* 10 (1997) 38–43.
- [49] K.D. Rice, R.D. Tanaka, B.A. Katz, R.P. Numerof, W.R. Moore, Inhibitors of tryptase for the treatment of mast cell-mediated diseases, *Curr. Pharm. Des.* 4 (1998) 381–396.
- [50] G.T. De Sanctis, M. Merchant, D.R. Beier, R.D. Dredge, J.K. Grobholz, T.R. Martin, E.S. Lander, J.M. Drazen, Quantitative locus analysis of airway hyperresponsiveness in A/J and C75BL/6J mice, *Nature Genet.* 11 (1995) 150–154.
- [51] J.E. Hunt, R.L. Stevens, K.F. Austen, J. Zhang, Z. Xia, N. Ghildyal, Natural distribution of the mouse mast cell protease 7 gene in the C57BL/6 mouse, *J. Biol. Chem.* 271 (1996) 2851–2855.
- [52] J. Stürzebecher, D. Prasa, C.P. Sommerhoff, Inhibition of mast cell tryptase by benzamidine derivatives, *Biol. Chem. Hoppe-Seyler* 373 (1992) 1025–1030.
- [53] G.H. Caughey, W.W. Raymond, E. Bacci, R.J. Lombardy, R.R. Tidwell, Bis(5-amidino-2-benzimidazolyl)methane and related amidines are potent, reversible inhibitors of mast cell tryptases, *J. Pharmacol. Exp. Ther.* 264 (1993) 676–682.
- [54] L.E. Burgess, B.J. Newhouse, P. Ibrahim, J. Rizzi, M.A. Kashem, A. Hartman, B.J. Brandhuber, C.D. Wright, D.S. Thomson, G.P.A. Vigers, K. Koch, Potent selective nonpeptidic inhibitors of human lung tryptase, *Proc. Natl. Acad. Sci. USA* 96 (1999) 8348–8352.
- [55] S. Ono, S. Kuwahara, M. Takeuchi, H. Sakashita, Y. Naito, T. Kondo, Synthesis and evaluation of amidinobezofuran derivatives as tryptase inhibitors, *Bioorg. Med. Chem. Lett.* 9 (1999) 3285–3290.
- [56] K.D. Rice, A.R. Gangloff, E.Y.-L. Kuo, J.M. Dener, V.R. Wang, R. Lum, W.S. Newcomb, C. Havel, D. Putnam, L. Cregar, M. Wong, R.L. Warne, Dibasic inhibitors of human mast cell tryptase. Part 1: Synthesis and optimization of a novel class of inhibitors, *Bioorg. Med. Chem. Lett.* 10 (2000) 2357–2360.
- [57] K.D. Rice, V.R. Wang, A.R. Gangloff, E.Y.-L. Kuo, J.M. Dener, W.S. Newcomb, W.B. Young, D. Putnam, L. Cregar, M. Wong, P.J. Simpson, Dibasic inhibitors of human mast cell tryptase. Part 2: Structure-activity relationships and requirements for potent activity, *Bioorg. Med. Chem. Lett.* 10 (2000) 2361–2366.
- [58] C.P. Sommerhoff, C. Söllner, R. Mentele, G.P. Piechottka, E.A. Auerswald, H. Fritz, A Kazal-type inhibitor of human mast cell tryptase: Isolation from the medical leech *Hirudo medicinalis*, characterization, and sequence analysis, *Biol. Chem.* 375 (1994) 685–694.
- [59] J.F. Morrison, Kinetics of the reversible inhibition of enzyme-catalysed reactions by tight-binding inhibitors, *Biochim. Biophys. Acta* 185 (1969) 269–286.